Applied Surface Science xxx (2013) xxx–xxx

Contents lists available at SciVerse ScienceDirect

Applied Surface Science

journal homepage: www.elsevier.com/locate/apsusc

Degradation and modification of stainless-steel surface using Cl_2/Ar inductively coupled plasma

Hanbyeol Jang[a], Alexander Efremov[b], Sun Jin Yun[c], Geun Young Yeom[d], Kyoung Bo Kim[e], Kwang-Ho Kwon[a,*]

[a] Dept. of Control and Instrumentation Engineering, Korea University, 2511 Sejong-Ro, Republic of Korea
[b] Dept. of Electronic Devices & Materials Technology, State University of Chemistry & Technology, 7 F. Engels st., 153000 Ivanovo, Russia
[c] Electronic and Telecommunications Research Institute, Daejon 305-350, Republic of Korea
[d] Dept. of Advanced Materials Science & Engineering, Sungkyunkwan University, Suwon 440-746, Republic of Korea
[e] POSCO Global R&D Center, Open Innovation Lab., Incheon 406-840, Republic of Korea

ARTICLE INFO

Article history:
Received 1 November 2012
Received in revised form 5 March 2013
Accepted 29 March 2013
Available online xxx

Keywords:
Stainless-steel
Cl_2/Ar plasma
Etching
Modification
Roughness
Free surface energy

ABSTRACT

The investigations of stainless steel (SS) etching behavior in the Cl_2/Ar inductively coupled plasma as well as the etched surface characteristics were carried out. It was found that an increase in Ar fraction in the Cl_2/Ar plasma from 0 to 100% at fixed gas pressure, input power and bias power results in decreasing both etching (degradation) rate of the SS surface (41.3–1.5 nm/min) and mean SS surface roughness (84–20 nm). Plasma diagnostics by Langmuir probes and 0-dimensional plasma modeling provided the data on plasma parameters, steady-state densities and fluxes of active species on the etched surface. It was shown that the maximum changes in mean roughness as well as in both polar and dispersive components of free surface energy correspond to a maximum value of Cl atom flux/ion flux ratio. Also, the linear correlation between free surface energy and mean roughness was obtained.

1. Introduction

During the last decade, many new materials have been involved in the electronic device technology. Particularly, the stainless-steel (SS) foil has been tested instead of the rigid glass substrate in the Cu(In,Ga)Se_2 (CIGS) solar cells technology [1–4]. The advantage of SS foil substrates is the flexibility that allows one to use the roll-to-roll manufacturing and thus, to reduce the device cost [1,2]. At the same time, the main drawback of the SS substrate is the pure adhesion to various functional layers deposited above and namely, to Mo or Mo/Ti layers [1]. Therefore, the problem of adhesion for the SS foil surface is an important task to be solved for improving solar cell characteristics.

From Refs. [5–8], it is known that the properties of both organic and inorganic surfaces can be modified by plasma treatment. The meaning of "modification" includes many effects such as the change of surface morphology, roughness and/or chemical composition while the properties of treated (or etched, in the case of chemically active plasmas) surface can be very different compared with both original surface and bulk material. Particularly, the parameter of our interest – the adhesion ability – is linked with the free surface energy [5] that should be optimized to a maximum value. At the same time, free surface energy depends on both surface roughness and chemical state [5,8].

Until now, there are no works devoted to the investigation of the SS modification characteristics and mechanisms in both noble gas and chemically active gas plasmas. There are only some occasional mentions that this material is quite stable to the halogen-containing plasma exposure, so that it is frequently used for plasma etching equipment manufacturing [5,7]. Therefore, the lack of data on the SS degradation and modification in chemical and physical etching processes retards the improvement of the solar cell technology.

The aim of present work was to investigate the SS etching (degradation) mechanism in the Cl_2/Ar inductively coupled plasmas as well as to find out the interconnections between plasma parameters and etched surface characteristics. The Cl_2/Ar mixing ratio was chosen as the single variable because it provides the clear transition between chemical and physical etching pathways and thus, allows one to analyze the features and the impacts of these principal regimes. For this purpose, a combination of plasma diagnostics, plasma modeling and surface investigation methods was applied.

* Corresponding author. Tel.: +82 44 860 1447; fax: +82 44 865 1820.
E-mail address: kwonkh@korea.ac.kr (K.-H. Kwon).

0169-4332/$ – see front matter © 2013 Elsevier B.V. All rights reserved.
http://dx.doi.org/10.1016/j.apsusc.2013.03.175

2. Experimental and modeling details

Etching and plasma diagnostic experiments were performed in a planar inductively-coupled plasma (ICP) reactor. The reactor had a cylindrical chamber (r = 16 cm) made from anodized aluminum and a 5-turn copper coil located above a 10-mm-thick horizontal quartz window. The coil was connected to a 13.56-MHz power supply. The distance (l) between the window and the bottom electrode that was used as a substrate holder was 12.8 cm. The bottom electrode was connected to a 12.56-MHz power supply in order to maintain a negative DC bias voltage. The experiments were performed with fixed gas pressure (p = 6 mTorr) input power (W_{inp} = 1000 W) and bias power (W_{dc} = 350 W). The Cl_2/Ar mixing ratio was varied from 0 to 100% Ar by adjusting the partial flow rates of pure gases within the total flow rate of 50 sccm. The SS samples with the size of 2 cm × 2 cm and the thickness of about 100 μm were placed at the center of the bottom electrode. The temperature of the bottom electrode was stabilized at 17 °C using a water-flow cooling system.

The SS etched depths were measured using a surface profiler (Alpha-step 500, Tencor). For this purpose, we developed the line striping of the photoresist (AZ1512, positive) with the line width/spacing ratio of 2 μm/2 μm. The SS surface morphology was investigated using the atomic force microscope (AFM-XE100, Park system). The data on mean surface roughness were obtained using the software supplied by the equipment manufacturer. Free surface energy was calculated through the Owens–Wendt equation [9]. For this purpose, the measurements of contact angles with polar (deionized water) and non-polar (CH_2I_2) liquids were provided using the drop shape analysis system (DSA-100, KRUSS).

Plasma diagnostics were performed using a double Langmuir probe (DLP2000, Plasmart Inc.). The probes were installed through the viewport on the sidewall of the reactor chamber, at a point that was 5.7 cm above the bottom electrode and centered in a radial direction. The treatment of I–V curves to obtain electron temperature (T_e) and total positive ion density (n_+) was carried out using the software supplied by the equipment manufacturer. Calculations were performed based on Johnson and Malter's double probe theory [10] and by using the Allen-Boyd-Reynolds approximation, the ion-saturation current density was applied.

In order to obtain the data on plasma parameters and fluxes of plasma active species, we used a simplified global (zero-dimensional) model with a Maxwellian approximation for the electron energy distribution function (EEDF) [11–13]. The experimental data on T_e and n_+ were directly applied as input model parameters. The simultaneous solutions of (1) the steady-state balanced equations for neutral and charged species and (2) the quasi-neutrality conditions for both bulk plasma and plasma–surface interface provided the data on volume-averaged densities of the rest charged species (electrons, negative ions), neutral ground-state species (Cl_2 and Cl) as well as the fluxes of all these species on the treated surface. The details about the algorithm, reaction set and the rest input data are given in Refs. [14,15].

3. Results and discussion

When a combination of chemically active gas and noble gas is used for the material etching, the behavior of the etching rate with operating parameters as well as the properties of the etched surface depends strongly on the contributions of chemical and physical etching pathways. Among the main SS surface components (15.24% Fe, 9.59% Cr, 2.99% Mn, 25.3% O, 40.29% C, 2.15% N and 3.44% Si), there are no metals forming the volatile chlorides at near-to-room temperatures. This directly follows from the analysis of boiling points (T_{bp}) for corresponding compounds: T_{bp} = 1023 °C for $FeCl_2$, 326 °C for $FeCl_3$, 1300 °C for $CrCl_3$, >600 °C for $CrCl_4$, 1190 °C for $MnCl_2$ and 57.6 °C for $SiCl_4$ [16]. Note that the formation of $SiCl_4$ in the crystal structures is retarded by the low penetration of the Cl atoms inside the lattice, so that the much lower volatile $SiCl_2$ is the dominant reaction product [7,8]. As a result, the spontaneous etching of the SS surface at temperatures below 100 °C can be neglected due to the formation of the quite stable protective layer composed from the non-volatile metal chlorides. That is why the SS is a widely used material for plasma etching reactors and pumping equipment working with the chlorine-containing plasmas [5,7]. The etching of the SS surface takes place only with the strong ion bombardment which removes the reaction products and thus, provides the development of chemical reaction. Therefore, the SS etching mechanism in the Cl_2/Ar plasma can be pre-determined as the ion-assisted chemical reaction.

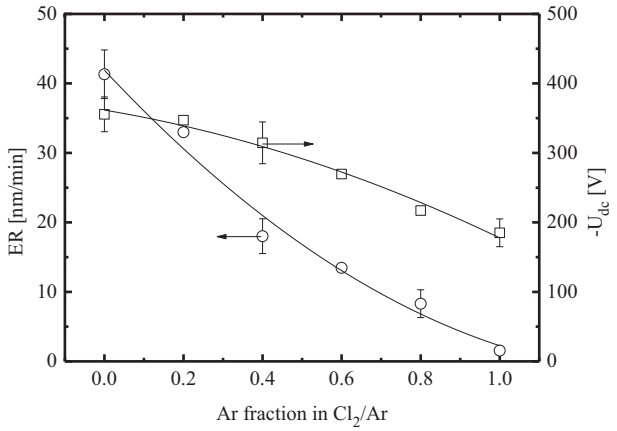

Fig. 1. Stainless steel etching rate (ER) and negative dc bias voltage ($-U_{dc}$) as functions of Cl_2/Ar mixing ratio at p = 6 mTorr, W = 1000 W and W_{dc} = 350 W. The solid lines are to guide the eye only.

Fig. 1 illustrates the influence of gas mixing ratio on the SS etching rates as well as on the negative ds bias at W_{dc} = const. It can be seen that, as the Ar fraction increases from 0 to 100%, the SS etching rate decreases monotonically in the range of 41.3–1.6 nm/min, i.e. by more than 25 times. This allows one to make an assertion that, for the given process conditions, the chemical etching pathway is more effective than the physical one. However, an exact conclusion on the SS etching mechanism as well as the further analysis of the etched surface characteristics requires the data on plasma parameters and fluxes of active species.

The detailed analysis of plasma parameters and chemistry in Cl_2/Ar ICP has been performed in our works [14,15]. Below, we would like to focus the attention only on the key issues which are important for the purpose of this research.

An increase in T_e with increasing Ar mixing ratio (2.5–2.9 eV for 0–100% Ar, see Fig. 2(a)) is in agreement with published data and is connected with the lower electron energy losses for the excitation and ionization of Ar atoms [15,17]. This results in increasing rate coefficients for electron impact processes, and mainly for the high-threshold ionizations. Accordingly, the growth of measured n_+ (1.1×10^{11}–7.0×10^{11} cm^{-3} for 0–100% Ar) and model-predicted n_e (4.9×10^{10}–7.0×10^{11} cm^{-3} for 0–100% Ar) is associated with an increase in the total ionization rate as well as with the change in the total charge balance due to decreasing negative ion density. Both total flux of positive ions Γ_+ (3.5×10^{15}–3.7×10^{16} cm^{-2} s^{-1} for 0–100% Ar) and the ion saturation current density J_+ (2.5–17.9 mA/cm^2 for 0–100% Ar, see Fig. 2(b)) follow the behavior of n_+ which is also supported by increasing ion Bohm velocity. From Refs. [6,18–20], it can be understood that the efficiency of ion bombardment can be generally characterized by $m_i(\varepsilon_i)^{1/2}\Gamma_+$ where m_i is the effective ion mass,

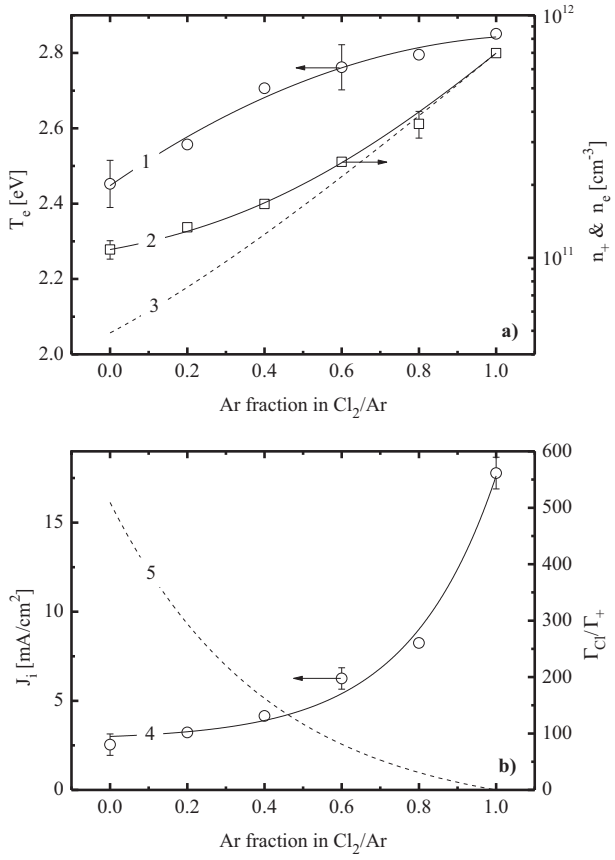

Fig. 2. Measured (solid lines + symbols) and model-predicted (dashed lines) plasma parameters as functions of Cl_2/Ar mixing ratio: 1 – electron temperature, 2 – total positive ion density, 3 – electron density, 4 – ion saturation current, 5 – neutral/charged ratio. The conditions correspond to Fig. 1.

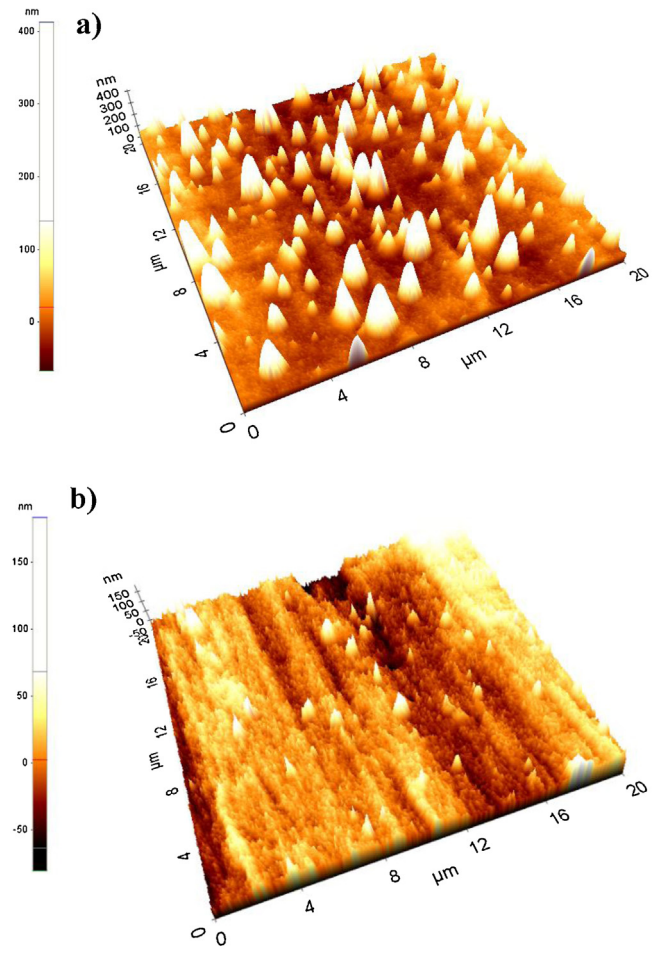

Fig. 3. AFM images of the stainless steel surfaces treated in Cl_2-rich (80% Cl_2 + 20% Ar, (a) and Ar-rich (20% Cl_2 + 80% Ar, (b) plasmas. The conditions correspond to Fig. 1.

and ε_i is the ion bombardment energy. High dissociation degrees for Cl_2 molecules (n_{Cl}/n_{Cl_2} = 5–38 for 0–80% Ar) provide the domination of Cl^+ over Cl_2^+, so that $m_i \approx$ const for 0–100% Ar because of $m_{Cl^+} \approx m_{Ar^+}$. The ion bombardment energy is $\varepsilon_i \approx e|-U_{dc} - U_f|$, where $U_f \approx 6\,T_e$ is the floating potential [18], and U_{dc} is the negative dc bias from an external power source (Fig. 1). In our case, the variation of $(\varepsilon_i)^{1/2}$ (19.2–14.2 $eV^{1/2}$ for 0–100% Ar) is much weaker than that for Γ_+ and thus, does not influence principally the behavior of $(\varepsilon_i)^{1/2}\Gamma_+$. Therefore, the impact of the physical etching pathway on the modification of the SS surface can be characterized by the Γ_+ only.

Though the addition of Ar increases the dissociation efficiency for Cl_2 molecules ($k_{dis}n_e$ = 795–6310 s^{-1} for 0–80% Ar), this effect is completely compensated by decreasing n_{Cl_2}. As a result, both Cl atom density ($n_{Cl} = 1.4 \times 10^{14}$–$3.7 \times 10^{13}$ cm^{-3} for 0–80% Ar) and Cl atom flux ($\Gamma_{Cl} = 1.8 \times 10^{18}$–$1.9 \times 10^{17}$ $cm^{-2}\,s^{-1}$ for 0–80% Ar) follow the Cl_2 fraction in the Cl_2/Ar mixture. Generally, the efficiency of the chemical etching pathway can be y characterized by $\gamma_R\Gamma_{Cl}$ [19,20], where γ_R is the reaction probability. Since, in our case, $\gamma_R \approx$ const because of constant surface temperature, the impact of the chemical etching pathway on the modification of the SS surface is controlled by the Γ_+ only.

From the above data, one can conclude that the parameter Γ_{Cl}/Γ_+ (so-called, neutral/charged ratio) directly characterizes the balance between chemical and physical impacts on the SS surface. In order to figure out the SS etching mechanism, it is reasonable to analyze the correlations of the SS etching rate with both Γ_{Cl} and Γ_+ as well as the interconnections between neutral/charged ratio and the SS surface characteristics. The comparison of Figs. 1 and 2(b) show that the behavior of the SS etching rate contradicts with Γ_+, but follows Γ_{Cl}. Such situation formally corresponds to the reaction-rate-limited etching regime. In our case, such regime can take place only if the ion bombardment provides enough cleaning of the SS surface from the low volatile reaction products. Particularly, from Ref. [18], it can be understood that the reaction-rate-limited regime in Cl_2/Ar ICP under the close range of operating conditions starts when the fraction of free (not covered by the reaction product) surface exceeds 50–60%. Accordingly, the ion bombardment energy (and thus, W_{dc}) seems to be the key parameter determining the regime of the whole SS etching process for the fixed Cl_2/Ar mixture composition.

From Figs. 3 and 4(a), it can be seen that an increase in Ar fraction and a decrease in neutral/charge ratio causes a sufficient decrease in surface roughness. Really, the mean roughness (MR) derived from the AFM images falls from 83.9 nm in pure Cl_2 plasma down to 19.7 nm in pure Ar plasma. The fact that the MR value increases with the Γ_{Cl}/Γ_+ ratio suggests that this effect has a chemical nature. In our opinion, it can be connected with, at least, two reasons. First, since an increase in Γ_{Cl}/Γ_+ is also escorted by increasing SS etching rate, the re-deposition of etch by-products is rather expectable. An indirect proof is that the MR and the SS etching rate demonstrate a not bad correlation (Fig. 4(a)). Here, the saturations of both etching rate and MR toward higher Γ_{Cl}/Γ_+ values may results from the saturation of the treated surface by the reaction products up to the limit determined by the total amount of active surface sites. Similar effects have repeatedly been reported for many materials used in micro- and nano-electronics technology [5,6]. And secondly, the

Please cite this article in press as: H. Jang, et al., Degradation and modification of stainless-steel surface using Cl_2/Ar inductively coupled plasma, Appl. Surf. Sci. (2013), http://dx.doi.org/10.1016/j.apsusc.2013.03.175

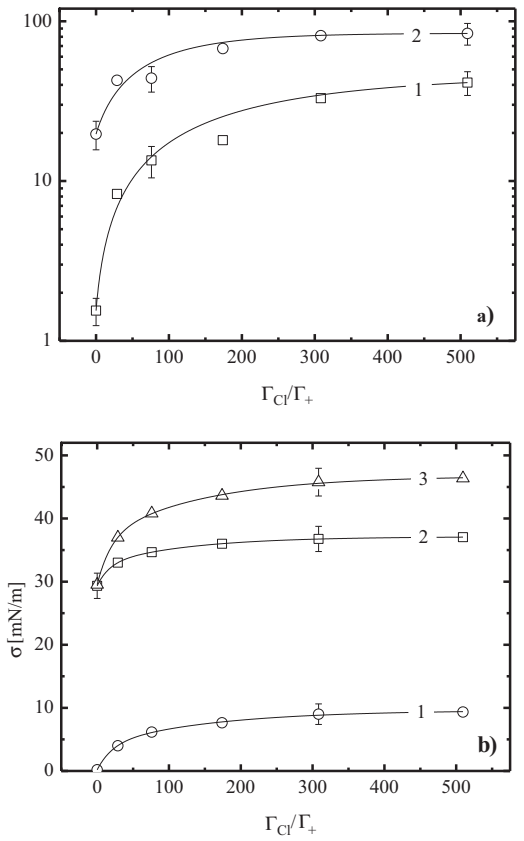

Fig. 4. Stainless steel surface characteristics as functions of neutral/charged ratio. In (a): 1 – etching rate, 2 – mean roughness (MR). In (b): 1 – dispersive, 2 – polar and 3 – total surface energy. The conditions correspond to Fig. 1.

domination of the chemical etching pathway at high Γ_{Cl}/Γ_+ ratios can result in the non-uniform surface degradation because of different partial etching (gasification) rates for SS components. In this case, the saturation of MR may be attributed to the limited penetration depth of Cl atoms inside the lattice. We also believe that both proposed mechanism do work together, and their contributions cannot be divided accurately within this study.

From Refs. [9,21], it is known that many surface characteristics (chemical activity, wettability, adhesion ability) are closely linked with the free surface energy (σ_T). Speaking simply, the higher σ_T values correspond to "active" surface while the lower σ_T allows one to speak about an "inert" surface. From Fig. 4(b), it can be seen that an increase in Γ_{Cl}/Γ_+ ratio causes an increase in both polar σ_P (29.3–37.0 mN/m, i.e. by 1.3 times for 0–100% Cl_2) and dispersive σ_D (0.2–9.3 mN/m, i.e. by 50 times for 0–100% Cl_2) components of surface energy, so that $\sigma_T = \sigma_P + \sigma_D = 29.5–46.4$ mN/m. The values of σ_P and σ_D for the original untreated SS samples are 24.1 mN/m and 0.2 mN/m, respectively. In our opinion, the change in σ_P directly results from increasing MR while a much smaller relative growth of σ_D can be associated with the change in chemical composition of etched surface. Particularly, since σ_D is generally determined by polar groups located on the surface, an increase in this parameter may result from increasing density of the original groups (mainly O-containing groups as the SS surface components and adsorbed gases) and/or from the formation of new groups with higher electron affinities. In our opinion, the last mechanism looks more reasonable. Probably, an increase in Γ_{Cl}/Γ_+ ratios causes the enrichment of the etched surface by the Cl-containing compounds through both re-deposition of etching by-products and localization of Cl atoms in the non-volatile metal chlorides. The saturations of σ_P and σ_D toward high neutral/charged rations may be

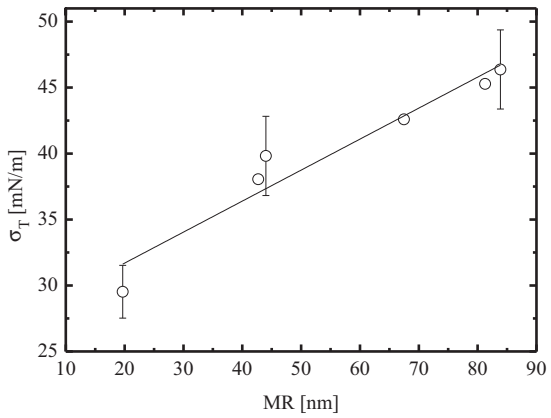

Fig. 5. Correlation between total surface energy and mean roughness. The conditions correspond to Fig. 1.

connected with the same reasons as was proposed for etching rate and surface roughness. Fig. 5 shows also that a not bad linear correlation between free surface energy and surface roughness takes place.

4. Conclusion

In this work, we carried out an investigation of SS etching behavior and surface characteristics using the Cl_2/Ar inductively coupled plasma. It was found that an increase in Ar fraction in the Cl_2/Ar plasma from 0 to 100% at fixed gas pressure, input power and bias power results in decreasing SS etching (degradation) rate (41.3–1.5 nm/min), mean surface roughness MR (84–20 nm) and free surface energy (46.4–29.5 mN/m). The data on plasma parameters and fluxes of plasma active species were obtained from a combination of plasma diagnostics by Langmuir probes and plasma modeling. It was shown that the SS etching kinetics correspond to the reaction-rate-limited etching regime while the maximum values of MR and σ_T correspond to higher Γ_{Cl}/Γ_+ ratios. Also, the linear correlation between σ_T and MR was obtained. All these allows one to conclude that treatment of the SS at higher Γ_{Cl}/Γ_+ ratios (an thus, at a domination of chemical etching pathway) provides more "active" surface and, probably, improves the adhesion characteristics for deposited layers.

Acknowledgment

This work was supported by the Industrial Strategic Technology Development Program (10041681, Development of fundamental technology for 10 nm process semiconductor and 10 G size large area process with high plasma density and VHF condition) funded by the Ministry of Knowledge Economy (MKE, Korea)

References

[1] F. Pianezzi, A. Chirila, P. Blösch, S. Seyrling, S. Buecheler, L. Kranz, C. Fella, A.N. Tiwari, Progress in Photovoltaics: Research and Applications (2012), DOI: 10.1002/pip.1247.
[2] C.Y. Shi, Y. Sun, Q. He, F.Y. Li, J.C. Zhao, Solar Energy Materials & Solar Cells 93 (2009) 654.
[3] Y. Hashimoto, T. Satoh, S. Shimakawa, T. Negami, Proceedings of the 3rd World Conference on Photovoltaic Energy Conversion, Osaka, Japan, 2003, 574.
[4] S. Niki, M. Contreras, I. Repins, M. Powalla, K. Kushiya, S. Ishizuka, K. Matsubara, CIGS Progress in Photovoltaics: Research and Applications 18 (2010) 453.
[5] J.R. Roth, Industrial plasma engineering Applications to Nonthermal Plasma Processing, vol. 2, IOP Publishing, Philadelphia, 2001.
[6] B. Chapman, Glow Discharge Processes: Sputtering and Plasma Etching, John Wiley & Sons, New York, 1980.
[7] M. Sugavara, Plasma Etching: Fundamentals and Applications, Oxford University Press, New York, 1998.

[8] M.A. Lieberman, A.J. Lichtenberg, Principles of Plasma Discharges and Materials Processing, John Wiley & Sons Inc., New York, 1994.
[9] M. Żenkiewicz, Journal of Achievements in Materials and Manufacturing Engineering 24 (2007) 137.
[10] E.O. Johnson, L. Malter, Physical Review 80 (1950) 58.
[11] C. Lee, M.A. Lieberman, Journal of Vacuum Science and Technology A 13 (1995) 368.
[12] M.A. Lieberman, S. Ashida, Plasma Sources Science and Technology 5 (1996) 145.
[13] P.N. Wainman, M.A. Lieberman, A.J. Lichtenberg, R.A. Stewart, C. Lee, Journal of Vacuum Science and Technology A 13 (1995) 2464.
[14] A.M. Efremov, G.H. Kim, J.G. Kim, A.V. Bogomolov, C.I. Kim, Microelectronic Engineering 84 (2007) 136.
[15] A. Efremov, N.-K. Min, B.-G. Choi, K. -Ha Baek, K.-H. Kwon, Journal of the Electrochemical Society 155 (2008) D777.
[16] D.R. Lide, Handbook of Chemistry and Physics, CRC Press, New York, 1998–1999.
[17] M.V. Malyshev, V.M. Donnelly, Journal of Applied Physics 90 (2001) 1130.
[18] A.M. Efremov, D.P. Kim, C.I. Kim, IEEE Transactions on Plasma Science 32 (2004) 1344.
[19] H.W. Winters, J.W. Coburn, Surface Science Reports 14 (1992) 162.
[20] K.-H. Kwon, A. Efremov, M. Kim, N.K. Min, J. Jeong, K. Kim, Journal of the Electrochemical Society 157 (2010) H574.
[21] S. Kitova, M. Minchev, G. Danev, Journal of Optoelectronics and Advanced Materials 7 (2005) 249.

Please cite this article in press as: H. Jang, et al., Degradation and modification of stainless-steel surface using Cl_2/Ar inductively coupled plasma, Appl. Surf. Sci. (2013), http://dx.doi.org/10.1016/j.apsusc.2013.03.175